

## Theoretical studies on the photochromic processes of 4-bromo-N-salicylideneaniline

Wei-Hai Fang<sup>1</sup>, Xiao-Zeng You<sup>1</sup>, Zhen Yin<sup>2</sup>

<sup>1</sup> Coordination Chemistry Institute, The State Key Laboratory of Coordination Chemistry, Nanjing University, Center for Advanced Studies in Science and Technology of Microstructure, Nanjing 210093, P.R. China

<sup>2</sup> Department of Physics, Nanjing University, Nanjing, 210093, P.R. China

Received June 15, 1994/Final revision received March 20, 1995/Accepted March 20, 1995

**Summary.** In the present paper, we carry out a semiempirical SCF MO AM1 investigation on the photochromic mechanism of 4-Br-N-salicylideneaniline (BrSA). Optimized equilibrium geometries and the nature of the excited-state potential energy surfaces are consistent with experimental findings. The calculated excited-state potential energy profiles can semiquantitatively explain the experimental facts. The photochromic processes which are initiated by excitation of the enol form to its first excited singlet state  $S_1$  involve the proton transfer from the hydroxyl oxygen to the imine nitrogen via six-membered ring transition states. Theoretical studies show that the proton transfer from the  $S_1$  state produces the keto form either on excited singlet state  $S'_1$  or on triplet state  $T'_1$  which may further decay to the ground state via radiative or nonradiative processes. The ultimate product of the photochromic reaction is mainly *trans*-ketoamine with partial zwitterion character. All of these have been confirmed by the experiments.

**Key words:** AM1 method – Photochromism – 4-bromo-N-salicylideneaniline

### 1 Introduction

Aromatic Schiff bases, as the compound revealing photochromic properties, have been the subject of interest for more than three decades. The photochromism of 4-Br-N-salicylideneaniline in the crystalline state or in solution was experimentally established to be attributed to an excited state intramolecular proton transfer [1, 2]. Absorption and emission spectra of BrSA have been studied in polar and nonpolar solvents [3], the fluorescence maximum is red shifted over  $10\,000\text{ cm}^{-1}$  from the absorption maximum. In order to explain the fluorescence kinetics of BrSA, Barbara et al. proposed that the Franck–Condon vertically excited enol state underwent a tautomeric proton transfer producing an excited keto state which contains a substantial amount of excess vibrational energy. The excited keto state is reactive toward formation of *trans*-keto in the ground state, and also is rapidly converted to the ground state *cis*-keto by vibrational relaxation and radiation. It seems that there has been a controversy over the structure of photo-product. Cohen and Schmidt proposed a *trans*-quinoid structure in which the oxygen atom and the imine hydrogen atom are in *trans* position with respect to the

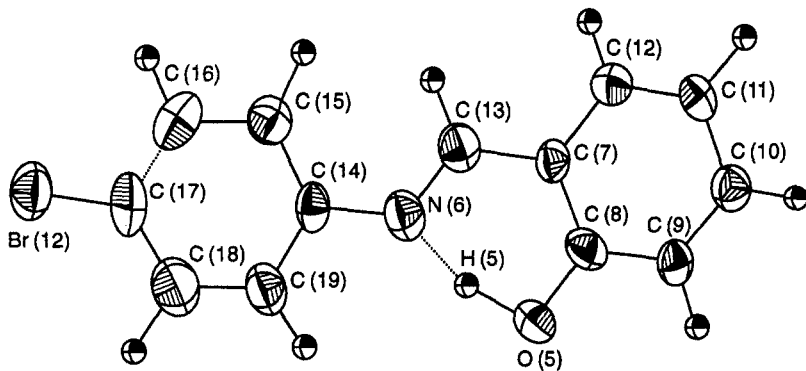


Fig. 1. Structures and atomic numbering of BrSA

C<sub>7</sub>-C<sub>13</sub> bond (Fig. 1). This idea has been supported by a number of subsequent studies [3-5]. The same quinoid structure but with a different nuclear configuration, a *cis*-quinoid structure, was suggested by Richey and Beeker [6]. Lewis and Sandorfy [7] proposed a zwitterion structure in which an intramolecular electron transfer occurs from the oxygen atom to the nitrogen atom. Therefore, theoretical studies on photochromic processes of the simple Schiff bases which, as far as we know, have not appeared in the literature yet, are of considerable interest. In this paper, we take 4-Br-N-salicylideneaniline (BrSA) as a typical example and make a theoretical study on its photochromic process. The structure of photoproduct is also discussed based on the semiempirical SCF MO AM1 calculations.

## 2 Computational method

For molecules in their excited electronic states, the most reliable results are obtained using *ab initio* methods with allowance for correlation energy. Such an approach, however, requires large basis sets and extensive configuration interaction, and is very costly in terms of computer time. Application of high quality *ab initio* techniques in theoretical studies on the mechanism of photoreaction has therefore so far been limited to small systems only. The AM1 method basically consists of an improved parametrization for the MNDO Hamiltonian, which has been optimized to reproduce a large set of ground-state data of organic molecules, ions and radicals [8]. In particular, the description of hydrogen bonds has been improved as compared with the original MNDO method [9]. In 1990, Dick has used the AM1 method to optimize the geometry of 3-hydroxyflavone in its crystal and pointed out that the root-mean-square difference in optimized and observed bond lengths is smaller than 0.02 Å [10]. Recently, the charge density wave and geometric soliton structures of  $\alpha, \omega$ -diphenyl odd polyene ions (C<sub>6</sub>H<sub>5</sub>)<sub>2</sub>(CH)<sub>2n+1</sub> ( $n = 10, 15, 20, \dots$ ) have been calculated with the AM1 method [11]. We have used the AM1 method to investigate photodecarboxylation reaction of acrylic acid [12]. The results obtained are qualitatively consistent with those of *ab initio* calculation [13], but the potential barrier calculated is higher than that of the CI calculation based on ROHF optimized structure. In the present paper, the geometrical parameters of stationary points on the ground-state and excited-state potential profiles

are optimized by using the AM1 method with an energy gradient technique. The SCF electron configuration of the ground state is  $(1a')^2 (2a')^2 \dots (1a'')^2 \dots (28a')^2 (12a'')^2 [(core)^{78} (12a'')^2]$ , whereas the electron configurations of the lowest electronically excited states are  $(core)^{78} (12a'')^1 (29a')^1$  for the enol form, and  $(core)^{78} (12a'')^1 (13a'')^1$  for the keto form. A crossing of the potential energy surfaces is probably involved in the photochromic processes. According to Morokuma's definition, the energy minimum crossing point between two potential surfaces corresponds to the point where the energy of one state is minimum under the constraint that the energies of two states are equal to each other [14]. We use a stepwise optimization method to locate such a crossing point between  $^1A''$  and  $^3A'$  excited state potential surfaces of BrSA. The calculations were performed with the GAUSSIAN 86 program [15].

### 3 Results and discussion

Before investigating the photochromism, we discuss on the possibility of the thermochromism of BrSA. The thermochromic reaction of BrSA involves an intramolecular proton transfer from the hydroxyl oxygen to the imine nitrogen, which is given at the bottom of Fig. 2.

For the thermochromic process, optimized geometrical parameters for the reactant [enol form ( $S_0$ )], the transition state ( $TS_0$ ) and the product [cis-keto form ( $S_0'$ )] are partially listed in Table 1. The potential profile of the thermochromic reaction is shown at the bottom of Fig. 3. From calculated potential barrier, 99 and 82  $\text{kJ mol}^{-1}$  for forward and backward reactions, it can be seen that the backward reaction is easier to proceed than the forward reaction at room temperature. The equilibrium ratio of cis-keto form and enol form at 300 K is evaluated as follows:

$$N_{\text{cis-keto}}/N_{\text{enol}} = k_+/k_- \approx \exp(-17280/RT) \approx 0.001,$$

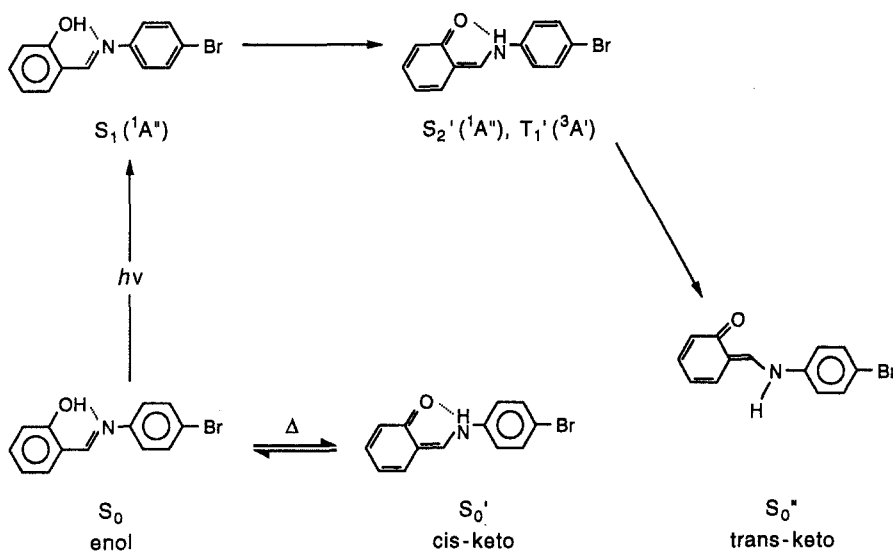


Fig. 2. Photochromism and thermochromism of BrSA

**Table 1.** Selected geometrical parameters of several stationary points on ground and excited potential profiles (bond length in Å, bond angles in degree)

	Ground state			Excited states				
	S <sub>0</sub>	TS <sub>0</sub>	S' <sub>0</sub>	S <sub>1</sub> ( <sup>1</sup> A'')	P	TSe ( <sup>1</sup> A'')	S' <sub>2</sub> ( <sup>1</sup> A'')	T' <sub>1</sub> ( <sup>3</sup> A')
C <sub>14</sub> -N <sub>6</sub>	1.407	1.399	1.403	1.284	1.362	1.369	1.416	1.415
C <sub>19</sub> -C <sub>14</sub>	1.416	1.415	1.418	1.460	1.426	1.426	1.411	1.421
C <sub>18</sub> -C <sub>19</sub>	1.389	1.389	1.388	1.381	1.391	1.391	1.393	1.393
C <sub>17</sub> -C <sub>18</sub>	1.398	1.399	1.398	1.411	1.404	1.404	1.394	1.399
Br <sub>12</sub> -C <sub>17</sub>	1.871	1.860	1.870	1.862	1.867	1.867	1.869	1.871
C <sub>13</sub> -N <sub>6</sub>	1.293	1.319	1.358	1.321	1.356	1.356	1.356	1.357
C <sub>13</sub> -C <sub>7</sub>	1.464	1.433	1.384	1.422	1.414	1.420	1.458	1.459
C <sub>9</sub> -C <sub>7</sub>	1.409	1.437	1.466	1.425	1.441	1.440	1.469	1.470
C <sub>6</sub> -C <sub>8</sub>	1.366	1.305	1.251	1.374	1.366	1.350	1.257	1.255
H <sub>5</sub> -O <sub>5</sub>	0.972	1.330	2.070	0.963	1.153	1.279	2.112	2.121
H <sub>5</sub> -N <sub>6</sub>	2.090	1.256	1.008	2.259	1.292	1.250	0.997	0.997
C <sub>9</sub> -C <sub>8</sub>	1.415	1.435	1.466	1.411	1.396	1.405	1.460	1.460
C <sub>10</sub> -C <sub>9</sub>	1.383	1.369	1.350	1.393	1.398	1.398	1.384	1.383
C <sub>11</sub> -C <sub>10</sub>	1.402	1.418	1.438	1.403	1.403	1.403	1.400	1.400
C <sub>12</sub> -C <sub>11</sub>	1.385	1.372	1.354	1.389	1.390	1.394	1.417	1.418
C <sub>15</sub> -C <sub>14</sub> -N <sub>6</sub>	125.16	123.79	123.34	121.89	120.94	120.94	120.48	120.53
C <sub>18</sub> -C <sub>19</sub> -C <sub>14</sub>	120.68	129.48	120.50	121.07	120.55	120.55	120.04	120.30
C <sub>17</sub> -C <sub>18</sub> -C <sub>19</sub>	120.53	120.59	120.57	120.99	120.53	120.53	119.98	120.26
Br <sub>12</sub> -C <sub>17</sub> -C <sub>18</sub>	120.25	120.51	120.28	120.17	120.14	120.14	121.04	120.03
C <sub>13</sub> -N <sub>6</sub> -C <sub>14</sub>	123.38	126.54	125.33	172.56	136.41	135.11	121.56	121.44
C <sub>7</sub> -C <sub>13</sub> -N <sub>6</sub>	123.50	119.69	125.74	128.57	119.11	119.82	124.38	124.24
O <sub>5</sub> -C <sub>7</sub> -C <sub>13</sub>	125.21	118.81	123.51	127.06	118.13	118.13	122.74	122.72
O <sub>5</sub> -C <sub>8</sub> -C <sub>7</sub>	125.65	121.26	122.76	125.52	119.31	119.81	123.32	123.23
H <sub>5</sub> -N <sub>6</sub> -C <sub>14</sub>	110.06 <sup>a</sup>	124.68	116.57	109.61 <sup>a</sup>	117.49	117.49	117.53	117.54
C <sub>9</sub> -C <sub>8</sub> -C <sub>7</sub>	120.36	117.97	116.66	120.93	121.09	120.49	117.24	117.00
C <sub>10</sub> -C <sub>9</sub> -C <sub>8</sub>	119.95	120.22	121.82	120.55	118.09	119.39	121.60	121.32
C <sub>11</sub> -C <sub>10</sub> -C <sub>9</sub>	120.26	121.41	120.92	119.90	120.69	120.69	120.54	120.26
C <sub>12</sub> -C <sub>11</sub> -C <sub>10</sub>	119.92	119.94	120.19	120.28	120.61	120.61	120.32	120.15
C <sub>13</sub> -N <sub>6</sub> -C <sub>14</sub> -C <sub>15</sub>	0.00	0.00	0.00	90.00	90.00	90.00	90.00	90.00
C <sub>7</sub> -C <sub>13</sub> -N <sub>6</sub> -C <sub>14</sub>	180.00	180.00	180.00	180.00	180.00	180.00	180.00	180.00

<sup>a</sup> H<sub>5</sub>-O<sub>5</sub>-C<sub>8</sub>

where  $k_+$  and  $k_-$  represent rate constants of the forward and backward reactions, respectively. All of these show that the system may be regarded to contain only a single component with all protons bound to the oxygen atoms at the temperature lower than 300 K. As pointed out by Hadjoudis et al. [4], a higher energy was required for proton transfer in the ground electronic state of BrSA; subsequently, no absorption attributable to the cis-keto form was observed at room temperature. The thermochromism of BrSA was also not observed by Cohen et al. [1]

The photochromic processes are initiated by excitation of the enol form to its first excited singlet state S<sub>1</sub>, followed by an intramolecular rotation. Then the proton transfers from the hydroxyl oxygen to the imine nitrogen via a six-membered ring transition state (Fig. 2), which is similar to the thermochromic reaction discussed above. The optimized structures of stationary points on excited-state potential profiles have a C<sub>s</sub> symmetry and the dihedral angle between the two

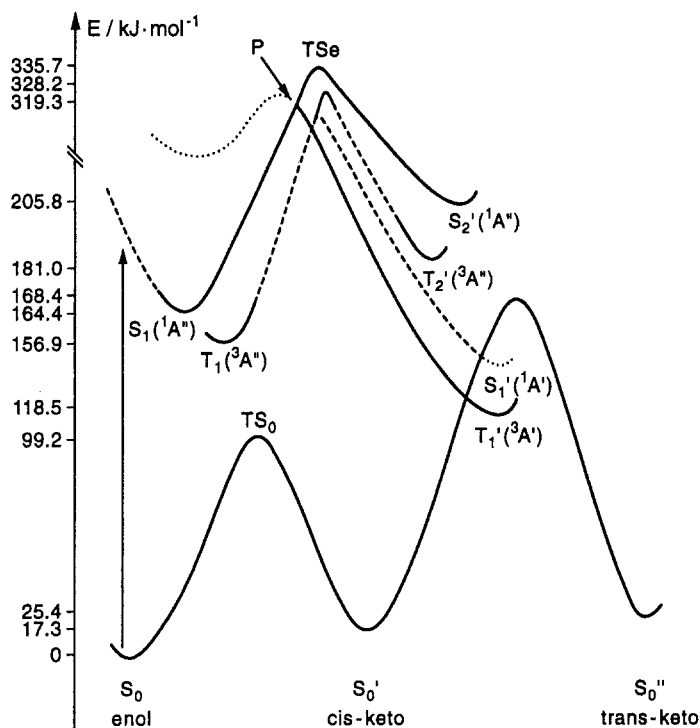
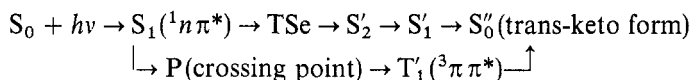


Fig. 3. Schematic potential profiles of reaction in low-lying electronic states of BrSA

aromatic groups of BrSA is  $90^\circ$ , which was supported by Rettig's discussion [16]. On the basis of molecular orbital coefficients and symmetries, the  $S_1$  state of the enol form is of  ${}^1n\pi^*({}^1A'')$  character, whereas the lowest excited triplet state of keto form ( $T_1'$ ) is of  ${}^3\pi\pi^*({}^3A')$  character, which is in agreement with the experimental assignment [17]. Geometrical parameters of some stationary points and the energy minimum crossing point ( $P$  point in Fig. 3) on the excited-state potential profiles are partially collected in Table 1. The potential profiles of the excited-state reactions are also depicted in Fig. 3 where relative energies of several stationary points are given. It can be seen from Fig. 3 that the population in the  $S_1$  state is transferred either to the second excited singlet state ( $S_2'$ ) of keto form along an adiabatic pathway (maintaining  ${}^1A''$  symmetry) or to the lowest excited triplet state ( $T_1'$ ) of the keto form via intersystem crossing. The zero-order energy minimum crossing point between  ${}^1A''$  and  ${}^3A'$  potential surfaces is determined with a stepwise optimization method. Because there exists spin-orbit interaction, the intersystem crossing is expected to take place in the vicinity of the crossing point [18]. This point can be considered as a "transition state" for nonadiabatic process  $S_1 \rightarrow T_1'$  [14], the potential barrier calculated ( $155 \text{ kJ mol}^{-1}$ ) is smaller than that of the adiabatic reaction  $S_1 \rightarrow S_2'$  ( $171 \text{ kJ mol}^{-1}$ ). It is well known that it is easy to relax from the high-energy  $S_2'$  state to the  $S_1'$  state. Taking into account that the intersystem crossing is spin-forbidden, it can be expected that the adiabatic and nonadiabatic processes represent competitive reaction pathways. Experiments

showed that proton transfer from the  $S_1$  state produces the keto form either on the excited singlet state  $S'_1$  surface [3] or on the excited triplet state  $T'_1$  ( $^3\pi\pi$ ) surface [17]. The dihedral angle between the quinoid group and the aniline group connected by the  $C_{13}$ - $N_6$  single bond is  $90^\circ$ , both in the equilibrium  $T'_1$  and  $S'_1$  structures. Therefore the quinoid group may rotate around the  $C_{13}$ - $C_7$  single bond more freely. These results show that there are two possible pathways for the excited  $S'_1$  and  $T'_1$  states to decay to the ground states, one of which results in the trans-keto form and the other results in the cis-keto form. The cis-keto form can easily transform back to the enol form, as discussed above. The barrier rotating from trans-keto to cis-keto was calculated to be  $143 \text{ kJ mol}^{-1}$ ; therefore the ground-state trans-keto is kinetically more stable. The photochromic processes may be represented as follows:



which is consistent with the photochromic mechanism proposed by Barbara et al. [3]. The analyses of Mulliken population on trans-keto form show that there are 4.5 electrons on the N atom and 6.3 electrons on the O atom (the two electrons in 1s orbitals are not included). This implies that the trans-keto form is of partial zwitterion character.

Experimental observations [3, 4] pointed out that the photochromism of BrSA could take place either in crystalline state or in solutions. Experiments in solvents of widely varying viscosities, from 0.22 cP for 2-methylbutane to the solid environment of crystalline nonadecane, show that the fluorescence kinetics of BrSA is only slightly affected. Solvent polarity over a limited range also seems to have little effect on the photochromism of BrSA; for example, the kinetics in polar ether are indistinguishable from the kinetics in nonpolar hydrocarbons. So the photochromic process of BrSA is mainly determined by an excited-state intramolecular proton transfer which has been elucidated by our AM1 calculations above. However, the intramolecular proton transfer may be influenced by intermolecular interactions. The intermolecular charge transfer interaction is generally considered to be an important factor [19] via which a change in the net charge on the atoms can occur. Such a charge effect has been found to have great influence on the nature of intramolecular proton transfer [4]. Another factor is the intermolecular force which will hinder the intramolecular rotation. The BrSA molecules are translationally stacked in the crystal which is a unique molecular crystal with intermolecular distance about 4.0 Å [1]. Such a structure provides weaker intermolecular force and intermolecular charge transfer interaction [20]. It is obvious that the intermolecular interaction has only a little influence on the photochromic mechanism of BrSA crystal. In solutions, the trans-keto form should be kinetically more stable as compared with the cis-keto form, since the calculated barrier of the trans-cis isomerization is higher in the ground state. This argument is supported by the recent NMR and time-resolved infrared spectra studies [21, 22]. However, the zwitterion character predicted by AM1 calculations is difficult to compare with experiments. Solvent polarity probably affects the structure of the ultimate photo-product as to whether it is quinoid or zwitterion. The extent of zwitterion character will vary with solvent polarity. As a general rule, the quinoid structure is favoured in nonpolar solvents and the zwitterion structure should be preferred in polar solvents.

*Acknowledgement.* This project was supported by the State Science and Technology Commission and National Natural Science Foundation of China.

## References

1. Cohen MD, Schmidt GMJ, Flavian S (1964) *J Chem Soc* 2042; Cohen MD, Schmidt GMJ (1962) *J Phys Chem* 66:2442
2. Hadjoudis E (1981) *J Photochem* 17:355
3. Barbara PF, Rentzepis PM, Brus LE (1980) *J Am Chem Soc* 102:2786
4. Hadjoudis E, Vittorakis M, Moustakali-Mavridis I (1987) *Tetrahedron* 43:1345
5. Turbeville W, Dutta PK (1990) *J Phys Chem* 94:4060
6. Richey WF, Beeker RS (1968) *J Chem Phys* 49:2092
7. Lewis JW, Sandorfy C (1982) *Can J Chem* 60:1738
8. Dewar MJS, Zoebisch EG, Healy EF, Stewart JJP (1985) *J Am Chem Soc* 107:3902
9. Dewar MJS, Thiel W (1977) *J Am Chem Soc* 99:4899
10. Dick B (1990) *J Phys Chem* 94:5752
11. Reimer JR, Craw JS, Hush NS (1993) *J Phys Chem* 97:1778
12. Fang W-H, Fang D-C, Liu R-Z (1993) *Acta Phys-Chim (in Chinese)* 9:788
13. Fang W-H, Fang D-C, Liu R-Z (1993) *Chinese Sci Bull* 38:1965
14. Koga N, Morokuma K (1985) *Chem Phys Lett* 119:371
15. Frisch MJ, Binkley JS, Schlegel HB, Raghavachari K, Melius CF, Martin RL, Stewart JJP, Bobrowicz FW, Rohlfing CM, Kahn LR, DeFrees DF, Seeger R, Whitesides RA, Fox DJ, Fleuder EM, Pople JA (1986) *GAUSSIAN 86*. Carnegie-Mellon Quantum Chemistry Publishing Unit, Pittsburgh, PA
16. Rettig W (1986) *Angew Chem Int Ed Engl* 25:971
17. Tero-Kubota S, Migita K, Akiyama K, Ikegami Y (1988) *J Chem Soc Chem Commun* 1067
18. Turro N (1978) *Modern molecular photochemistry*. Benjamin, Menlo Park
19. Inabe T, Gautier-Luneau I, Hoshino N, Okaniwa K, Okamoto H, Mttani T, Nagashima U, Maruyama Y (1991) *Bull Chem Soc Jpn* 64:801
20. Inabe T, Hoshino N, Mitani T, Maruyama Y (1989) *Bull Chem Soc Jpn* 61:4207
21. Turbeville W, Dutta PK (1990) *J Phys Chem* 94:4060
22. Yuzawa T, Takahashi H, Hamaguch H-O (1993) *Chem Phys Lett* 202:221